Research Article

Olabisi Theresa Ademosun*, Ernest C. Agwamba, Iqrar Ahmad, Harun Patel, Hitler Louis, Abiodun Humphrey Adebayo, Kolawole Oluseyi Ajanaku

Cytotoxic and phytochemical screening of *Solanum lycopersicum–Daucus carota* hydro-ethanolic extract and *in silico* evaluation of its lycopene content as anticancer agent

https://doi.org/10.1515/chem-2023-0164
received August 9, 2023; accepted October 6, 2023

Abstract: This article explores the potential of a specific functional food mix containing lycopene, a pigment found in tomatoes, for its role in cervical cancer prevention and treatment. The article assesses the cytotoxic effects on cervical cancer cells and conducts molecular docking analysis to understand the biological activities and binding interactions of lycopene. The formulations are analysed for their phytochemical profile, and their *in vitro* antioxidant activities are evaluated using spectrophotometric methods. Cytotoxicity tests on cervical cancer cells demonstrate that the ethanol extract of tomatoes exhibits the highest cytotoxic inhibition (40.28%), while carrots show minimal cytotoxic effects. Moreover, the lycopene extract exhibits dose-dependent cytotoxicity, with the highest concentration (1,000 µg/mL) displaying remarkable inhibition (74.2%). Molecular docking analysis indicates favourable interactions between lycopene and the pro-apoptotic protein BAX 1, suggesting its potential to induce apoptosis in cervical cancer cells, but camptothecin demonstrated stronger interactions. Molecular dynamics simulations confirm the stability of lycopene–protein complexes throughout the 100 ns simulation, supporting their potential as anticancer agents. Overall, the study highlights the cytotoxic effects of tomato–carrot food extracts and lycopene on cervical cancer cells. Molecular docking reveals the potential of lycopene to induce apoptosis through interactions with BAX 1. The stability analysis of lycopene–protein complexes further supports its anticancer properties. These findings enhance our understanding of the molecular mechanisms underlying the anticancer effects of lycopene and provide insights for future research on novel chemopreventive strategies for cervical cancer. However, further *in vivo* and clinical studies are warranted to validate the efficacy and safety of lycopene-based interventions.

Keywords: cervical cancer, tomato, carrot, lycopene, functional mix, cytotoxic, chemopreventive

*** Corresponding author: Olabisi Theresa Ademosun**, Chemistry Department, College of Science and Technology, Covenant University, Canaanland, Ota, Nigeria,
e-mail: olabisi.ademosun@covenantuniversity.edu.ng
Ernest C. Agwamba, Kolawole Oluseyi Ajanaku: Chemistry Department, College of Science and Technology, Covenant University, Canaanland, Ota, Nigeria
Iqrar Ahmad: Department of Pharmaceutical Chemistry, Prof. Ravindra Nikam College of Pharmacy, Gondur, Dhule, 424002, Maharashtra, India
Harun Patel: Division of Computer Aided Drug Design, Department of Pharmaceutical Chemistry, R. C. Patel Institute of Pharmaceutical Education and Research, Shirpur, 425405, Maharashtra, India
Hitler Louis: Computational and Bio-Simulation Research Group, University of Calabar, Calabar, Nigeria; Department of Pure and Applied Chemistry, University of Calabar, Calabar, Nigeria; Centre for Herbal Pharmacology and Environmental Sustainability, Chettinad Hospital and Research Institute, Chettinad Academy of Research and Education, Kelambakkam 603103, Tamil Nadu, India
Abiodun Humphrey Adebayo: Biochemistry Department, College of Science and Technology, Covenant University, Canaanland Ota, Nigeria

1 Introduction

Globally, in 2020, cancer was found responsible for about 10 million deaths. Each year, about 400,000 cases of cancer in children are diagnosed [1]. There are variations in the different cases of cancers in different countries, but cervical cancer was found to be the most common in 23 countries. Cancer has been identified as one of Nigeria's main causes of mortality. The high mortality rate among women in Nigeria has been attributed to diverse forms of cancer, such as breast, lung, cervical, and blood cancer [2]. Cancer arises because of malfunction or dysfunction that occurs in the human genetic makeup, and this makes cancer a genetic disease.

Some of the factors that trigger cancer are viruses, chemicals, and certain radiations. It is sometimes hereditary, and this can originate from any site in the human body, such as the case of gene mutations [3]. Normally, genes are responsible for the control of cell growth, cell division, and cell apoptosis, but an alteration in the activity of these genes, which is known as gene mutations, can result in the onset of cancer. Some of the cancer-causing gene mutations include the development of oncogenes which affects the cell division, survival, and multiplication of the cell; also, any alteration in the activity of tumour suppressor genes (genes that help keep the cell division and apoptosis in check) can lead to cells growing out of proportion which can contribute to the cancer risk factor. Cervical cancer is a form of cancer that originates from the cervix, the lower bottleneck of the uterus. Some of the factors that can predispose a woman to cervical cancer include Human Papilloma Virus, which is commonly transmitted via sexual intercourse [4]; sexual behaviours: men and women who have several sexual partners are more likely to develop cervical cancer [5]; smoking [6]; low supply of fruits and vegetables in the diet [7]; obesity [8]; and use of oral contraceptives for a long time and infection by chlamydia bacteria. In many low-income countries, women generally face a lot of burdens, such as economic, social, and health issues, and this also applies to women in Nigeria. This burden may be due to illiteracy, ignorance, and poverty as a result of their sexuality and childbearing activities. Currently, in Nigeria, the health priorities, according to the World Health Organization (2018) [9], are cancer, HIV/AIDS, tuberculosis, malaria, dysentery, pneumonia, and outbreaks of cholera and meningitis, which are on an occasional basis.

Furthermore, the World Health Organization (2018) confirms the fact that in Nigeria, the population of women between the ages of 15 years and above is 50.33 million, and these women are at high risk of developing cervical cancer. According to Kane et al. [10], a report showed that every year 14,943 women are diagnosed with this deadly disease, and 10,403 deaths are reported. Some of the bioactive compounds that have exhibited cytotoxicity on cervical cancer cell lines in the *in vitro* media include the essential oil of *Curcumin weyujin* [11], thymoquinone (2-isopropyl-5-methyle-1,4-benzoquinone) [12], tualang honey [13], lyophilized black raspberry extract [14], crude ethyl acetate extract from *Streptomyces cavouresis* KU-V39 [15], rosemary, turmeric, and ginger essential oils [16], Arabinogalactan (LBGP-I-3) [17], phenolics and flavonoids, and biotin-modified polylactic-*co*-glycolic acid nanoparticles [18,19].

Tomatoes are the third most important vegetable grown in the world and one of the most eaten fruits [20]. Tomato is not only sold as fresh fruit but can also be processed into a paste. It can be consumed in different ways; it can be eaten raw, as processed juice, in salads, and as ingredients for savoury meals [21]. It is rich in vitamin C, potassium, folate, antioxidants, carotenoids, flavonoids, and vitamin K, and it is free of cholesterol, which makes it an excellent dietary component [22]. In ripe tomatoes, phenolics and carotenoids are the main bioactive compounds, and most importantly, the red colour is due to the significant amount of lycopene in the fruit [22]. This berry fruit also contains β-carotene, which is known for its provitamin A activity [23]. In addition to the main bioactive compounds in tomatoes, vitamins, and glycoalkaloids are also present. Research has shown some major health benefits of carotenoids in tomatoes, such as protection against certain types of cancer [24–26], improves vision [27], prevents cardiovascular diseases [28], and improves sperm health [29]. The main bioactive component in tomatoes, lycopene, helps to prevent breast, prostate, liver, colon, and lung cancers [30,31]. Lycopene and other carotenoids are well-known for their antioxidant actions toward inhibiting free radical reactions. Lycopene provides an electron-rich system for electrophilic reagents, which enhances its performance and reactivity towards oxygen and free radicals; this can be attributed to the rich polyene structure of lycopene [32]. This active dietary antioxidant also acts as a viable oxygen-quenching agent by altering the reactions caused by free radicals like peroxyl radicals and OH^- [33]. Due to lycopene's conjugated polyene structure, rotary interactions with the solvent combined with vibrations can cause lycopene to lose the energy obtained during the process, resulting in the release of thermal energy. As the molecule quickly returns to its ground state, another O_2 quenching mechanism is engaged, allowing each carotenoid molecule to quench around 1,000 molecules of O_2 [32].

Carrot belongs to the Umbelliferae family, namely the genus Daucus and the species Carota. Carrots are known to be high in β-carotene, thiamine, and riboflavin [34]. Carrot consumption has been related to a variety of health advantages, including weight loss, cholesterol reduction, and improved eye health [35]. The seed of carrots has been found to possess antifungal, antibacterial, anti-inflammatory, analgesic, and cardio-hepatoprotective properties [36]. Carrots' numerous health advantages have been linked to their high consumption rate due to antioxidant and anticancer characteristics. It is extremely healthy, delicious, and crispy. It contains β-carotene, fibre, vitamins, antioxidants, and potassium [37]. The polyene structure of lycopene makes it a good target for electrophilic reagents because it provides an electron-rich environment for the reagents, resulting in maximal reactivity towards oxygen and free radicals [32].

The effect of carrot–tomato juice on humans was analysed to show whether food rich in carotenoids, most

especially high in β-carotene and lycopene, can help reduce the risk of colon carcinogenesis [38]. Bule and Singhal [39,40] showed that tomato juice and carrot juice increased the yield of ubiquinone-10 from 15.58 to 29.22 and 24.35 mg/L, respectively, when used as natural precursors.

Therefore, this article aimed at developing a functional food consisting of tomato and carrot as ingredients, its phytochemical assessment, *in silico* study on HeLa protein ligands, and *in vitro* cytotoxic assessment on cervical cancer human cell line (HeLa cells).

2 Materials and methods

2.1 Plant materials sampling

The naturally grown tomato and carrot fruits, which were naturally grown with no growth-promoting materials, were procured from a market in Ota, Ogun State, Nigeria. Ota is located at latitude 6.6882 °N and longitude 3.2347 °E. The plant materials were identified by Dr. J. O. Popoola, a taxonomist at Bowen University, Nigeria. Herbarium numbers were assigned, and a sample was stored in the herbarium of the university.

2.2 Production of tomato powder

Exactly 20 kg of matured tomatoes were fully cleaned in clean water to remove dirt and debris. The tomatoes were cut into smaller pieces using a kitchen knife to facilitate drying. The samples were oven-dried at a temperature of 60°C for 9 h till a uniform weight was attained. Using a mechanical blender, the dry materials were pulverized and stored at room temperature in a clean sterile glass container until further use.

2.3 Production of carrot powder

Ten kilograms of carrots were washed in clean water to remove dirt and debris. The outer layer of the carrots was peeled and cut into small pieces using a kitchen knife to facilitate drying. For 6 h, the samples were dried in an oven at 40°C. The dehydrated samples were powdered after being milled using a mechanical blender and stored at room temperature in a clean sterile container until further use.

2.4 Batch composition of tomato–carrot powder

The preparation of the formulation is presented in Table 1. Here, the mixtures were mixed thoroughly to ensure homogeneity.

2.5 Preparation of hydroethanolic extract of formulations

The milled samples (50 g) were soaked in 500 mL of 70% ethanol:30% water for 48 h of continuous agitation, and the resulting mixture was filtered using cheesecloth. The residues were soaked again in fresh solvents to enable total extraction. The filtrates were then pooled and filtered using filter paper (Whatman no. 1). A rotary evaporator was used to concentrate the filtrate, and the resulting residues were properly labelled and kept in a refrigerator at 4°C for future use.

2.6 Extraction of lycopene from *Solanum lycoperscicum*

Lycopene extraction was carried out using the modified method of Pandya [41]. The frozen pomace was taken from the deep freezer and thawed for 120 min before extraction. Lycopene extraction derived from tomato pomace was done using a shaker water bath. About 100 g of the pomace was placed into an iodine flask containing 1.5 L of the solvent (a combination of acetone and ethyl acetate in the ratio 2:1) and then placed on the flask rack of shaker water bath at 40°C for 5 h. This extraction method was used to extract lycopene from the plant matrix due to its insolubility in water-based solutions. The absorbance of the extract was read at 503 nm. The lycopene content (mg/100 g) was calculated using the following equation:

$$\text{Lycopene content} = \frac{A_{503}}{a_{503}} \times \frac{v}{100} \times \frac{100}{w}, \quad (1)$$

where A_{503} is the absorbance measured at 503 nm; a_{503} is the lycopene's specific extinction coefficient in *n*-hexane; v

Table 1: Batch composition of tomato–carrot powder

Samples	A	B	C	D	E	F	G
Tomato powder (%)	100	90	80	70	60	50	0
Carrot powder (%)	0	10	20	30	40	50	100

is the total solution volume, ml; and *w* is the weight of pomace (g).

3 Phytochemical analysis

3.1 Qualitative phytochemistry

The qualitative phytochemical screening for oxalate, quinone, terpenoid, cardiac glycoside, saponin, tannin, flavonoid, and alkaloid was evaluated using the method described by Varadharaj et al. [42]; briefly, 2 mL of ferric chloride (5%) was added to 1 mL of the extract. The presence of tannin was indicated by the formation of greenish-black colouration. For oxalate determination, a few drops of glacial ethanoic acid were applied to a 3 mL section of the extract. The presence of a greenish-black colouration indicated the presence of oxalate. About 1 mL of the extracts was treated with 1 mL of concentrated sulphuric acid, and the presence of quinones was indicated by the formation of red colouration. After adding 2 mL of chloroform to 1 mL of the extract, strong sulphuric acid was carefully added. The presence of terpenoids was shown by the production of brown colour at the interface. For phenol determination, 1 mL of the extracts was added to 2 mL of distilled water. After mixing, 10% of ferric chloride was added to the mixture dropwise. The presence of green coloration suggested phenol formation. About 2 mL of the extract was mixed with 2 mL of strong hydrochloric acid, followed by a few drops of Mayer's reagent. The presence of alkaloids in the extracts was indicated by the formation of green colouration. A mixture of 2 mL of glacial acetic acid and a few drops of ferric chloride (5%) was added to 500 µL of the extracts, after which 1 mL of concentrated H_2SO_4 was added to underlay the mixture. The formation of a brown ring at the interface indicated the presence of cardiac glycosides. In a tube, 2 mL of the extract and 2 mL of distilled water were added and agitated for 15 min. The presence of saponins in the extract was shown by the production of a 1 cm layer of foam. Before adding 5 mL of concentrated sulphuric acid, 5 mL of diluted ammonia solution was added to 10 mL of the sample. The production of yellow colouration in the sample suggested the presence of flavonoids.

3.2 Quantitative phytochemistry

The total phenolic content (TPC) was quantified using the method described by Sharma et al. [43]. Briefly, 2.7 mL of de-ionized water, 0.3 mL of extracts, 0.3 mL of 7 g/100 g 2.7 mL de-ionized water, 0.3 mL extracts, 0.3 mL 7 g/100 g Na_2CO_3, and 0.15 mL Folin–Ciocalteu reagent were carefully mixed, at 725 nm, the absorbance of the combination was measured. The absorbance of the mixture was measured at 725 nm. A gallic acid standard curve was prepared, and results were expressed as gallic acid equivalents (GAE) [44]. For the quantification of flavonoids in the extracts, the aluminium chloride colorimetric method described by Shraim et al. [45] was employed. In brief, 0.25 mL of the sample was diluted with distilled water to get 1.25 mL. There was 0.15 mL of aluminium chloride solution in 75 µL of 5% sodium nitrite. After 5 min, 0.5 mL of 0.1 M NaOH was added, followed by 2.5 mL of distilled water. The solution was properly mixed, and its absorbance at 510 nm was measured. A quercetin calibration curve was used to quantify the total flavonoid concentration, which was represented as milligram quercetin equivalents per gram dry weight was determined using the specified approach. Lycopene content was quantified as described by Davis et al. [46]. The quantification of lycopene was done using a spectrophotometer. β-Carotene was quantified as described by Alam et al. [47]. Briefly, the samples of interest were mixed with ethanol and heated for 5 min. The combination was sieved, and DCM was added with further heating for 4 min. A standard solution of β-carotene was prepared and was used to estimate the β-carotene in the sample spectrophotometrically. The total alkaloid was determined using the procedure specified by Li et al. [48].

4 Spectroscopic characterization of lycopene extract

The result shows that at 40°C and a ratio of 2:1 of acetone:ethylacetate, there was a yield of lycopene (4.34 mg/100 g). The extraction yield of lycopene in this research work is higher than the values obtained by some researchers who used different extracting solvents at different molar ratios, a mixture of hexane:acetone (3:1), which yielded 2.78 mg/100 g lycopene [49], hexane and ethanol, which yielded 3.58 and 1.25 mg/100 g lycopene, respectively. A better yield of 4.39 mg/100 g was recorded when ethyl acetate alone was used as the extracting solvent (Choi, 2012). The mixture of solvents with different polarities has been described to affect the extraction of bioactive compounds from plant materials, and this affects the total yield and also the phenolic components of the plant material [50]. Acetone and ethylacetate are polar aprotic solvents used in the extraction of lipophilic and hydrophilic substances. Polar aprotic solvents lack an acidic proton, and they are void of the hydroxyl (OH^-) group, which hinders the hydrogen

bonding reaction with the substrate. Tomatoes consist of a variety of lipophilic (carotenoids and vitamin E) and hydrophilic chemicals (vitamin C and phenolic compounds) and some volatile compounds; lycopene accounts for the most dominant lipophilic carotenoid in the tomato. The mixture of acetone and ethylacetate, two polar aprotic solvents, helped in the effective extraction of lipophilic lycopene, and a double portion of acetone gave a better yield of the carotenoid than a single molar ratio of acetone.

The spectral elucidation of the extracted lycopene was determined by ^{1}H and ^{13}C NMR. This was analysed at the Covenant University Bioinformatics Research Centre, Covenant University. The instrument used was from Nanalysis (Nanalysis NMReady v2.2.4.5, NMReady 60/analysis-X685). The ^{1}H and ^{13}C spectra were run at 60 and 15 Hz, respectively. Fourier transform infrared spectroscopy (FT-IR) (Perkin–Elmer FT-IR spectrophotometer) was used to analyse the extract molecular absorbance, composition, and structure. UV and gas chromatography–mass spectrometry (Agilent GC 7890B gas chromatography–mass spectrometry system, MSD 3977 A, USA) were analysed at the Covenant University Central Instrumentation Research (CUCIRF).

5 Cytotoxicity assessment

5.1 Cell treatment/3-(4,5-dimethylthiazol-2-yl)-2,5-diphenyltetrazolium bromide (MTT) assay

Treatment was done in 96-well microtiter plates with 99 µL of Dulbecco's modified Eagle medium (BioConcept) medium supplemented with 1% L-glutamine each (200 mM) and 5% foetal bovine serum and HeLa cells (a primary cervical carcinogenesis cell line). Serial drug dilutions ranging between 1,000 and 0.0001 µg/mL were done for the tomato extract, lycopene extract, negative control (group without any treatment drug), and the standard drug. Each treatment drug was added to the labelled well plates using a multi-micropipette in triplicate, and the four treatment groups were in one 96-well microtiter plate. After 24 h of incubation for effective cell proliferation (Temp. 37°C, CO_2), the plates were examined under an inverted microscope to confirm that the control and sterile conditions were met. About 10 µL of the MTT reagent was added to each well of the 96-well microtiter plates and incubated for 2 h; afterwards, 100 µL of DMSO was added to each of the wells containing the MTT reagent (Sigma-Aldrich) and incubated for 1 h after which the plate was read using a spectrophotometer (Thermo Scientific Varioskan Lux) at 570 and 630 nm. The inhibitory concentration (IC_{50}) values were considered by linear regression (Huber, 1993) from the dose inhibition curves using GraphPad Prism version 6.01. Camptothecin was used as the standard clinical drug [51].

5.2 Computational details

5.2.1 Molecular docking protocol

The binding score with the anti-apoptotic human BCL-2 protein (1G5M) (Petros et al. [52]; RCSB PDB IG5M) and pro-apoptotic (agonist) BAX 1 protein (4S0O) (Garner et al. [53]; RCSB PDB 4S0O) found in HeLa cell lines, in interaction with ligand and camptothecin as reference, was assessed. Using the Biovia discovery studio (Dassault Systèmes 2016), the proteins were produced by eliminating all water molecules, ligands, and heteroatoms. When the protein receptors were loaded into Molegro virtual docker (MVD), the defective amino acid was modified and optimized by providing the required charge and protonation (Molegro, 2013). When the protein's molecular surface was produced utilizing electrostatic surface type mapping, most of the five cavities were found using enlarged van der Waals force. Before importing campothecin (the standard drug) and lycopene (the sample drug) as ligands, the MVD software algorithm computed, identified, and assigned the protein charges and flexible torsions. Applying MolDock scoring (GRID), the docking of the ligands and receptor protein was established with a grid resolution of 0.30 and a binding site radius of 22 with the centre of point X: 3.36, Y: −4.29, and Z: 1.97. When the protein's molecular surface was produced utilizing electrostatic surface type mapping, most of the five cavities were found using enlarged van der Waals force. Before importing campothecin (the standard drug) and lycopene (the sample drug) as ligands, the MVD software algorithm computed, identified, and assigned the protein charges and flexible torsions. Applying MolDock scoring (GRID), the docking of the ligands and receptor protein was established with a grid resolution of 0.30 and a binding site radius of 22 with the centre of point X: 3.36, Y: −4.29, and Z: 1.97.

5.2.2 Molecular dynamics (MD) simulation study

The complex structure of lycopene with 1G5M and 4S0O proteins was obtained from the optimal docking conformation produced by molecular docking, and the Desmond Schrodinger programme was used to perform MD simulation with the OPLS3e force field (Tople et al. [54]). The ligand–protein complex was placed in a periodic orthorhombic box

Table 2: Qualitative phytochemical constituents of tomato–carrot hydroethanolic extract

Samples	Oxa.	Qui.	Terp.	Car. Gly.	Sap.	Tan.	Phen.	Flav.	Alk.
A_1	−	−	++	++	++	−	+	+	+
B_1	−	−	++	++	++	−	+	+	++
C_1	−	−	++	++	++	−	+	+	++
D_1	−	−	++	++	++	−	+	+	++
E_1	−	−	++	++	++	−	+	+	++
F_1	−	−	++	++	++	−	+	+	++
G_1	−	−	++	++	++	−	+	+	+

Key: −: Not detected, +: Moderately detected, ++: Detected. Subscript 1: 70% ethanol extract, Oxa – oxalate, Qui – quinones, Terp – terpenoids, Car. Gly – cardiac glycosides, Tan – tannins, Phen – phenol, Flav – flavonoids, Alk – alkaloids. A – 100% tomato powder; B – 90% tomato and 10% carrot; C – 80% tomato and 20% carrot; D – 70% tomato and 30% carrot; E – 60% tomato and 40% carrot; F – 50% tomato and 50% carrot; G – 100% carrot. The preliminary phytochemical analysis showed that oxalate, quinones, and tannins were not present in the ethanol extracts of the formulations.

with a 10 ns between the solute (SPC water) and the side of the box. The opposing ions (Na+ and Cl−) were given at a concentration of 0.15 M to neutralize the balance of the system. This solvated and neutral system underwent unconstrained energy reduction using a hybrid technique composed of the steepest descent and the limited-memory Broyden–Fletcher–Goldfarb–Shanno algorithms to resolve steric conflicts using a fixed parameter set from the OPLS3e force field.

The maximum number of iterations was set at 2,000, and the convergence criterion was set at 1.0 kcal mol^{-1} (Aljuhani et al. [55]; Radwan et al. [56]). After importing the generated minimized system (cms file) into the MD module, the simulation was run for 100 ns under an "isothermal-isobaric ensemble" (NPT) at a temperature of 300 K and a pressure of 1 bar. The "Nose–Hoover chain thermostat" and "Martyna–Tobias–Klein barostat" techniques were ensembled at 100 and 200 ps for isothermal–isobaric circumstances, respectively [57]. At 100 ps periods, simulation images were taken, and the outcomes of the trajectories were evaluated.

5.3 Statistical analysis

The data obtained from the qualitative, quantitative, and cytotoxic assessments were subjected to one-way analysis of variance with Duncan's *post hoc* test for all groups using Minitab [58]. At a 5% probability level, values were judged statistically distinct and 95% confidence level. The results were presented as mean ± SEM except otherwise stated.

6 Results and discussion

6.1 Phytochemical analysis

6.1.1 Qualitative phytochemical analysis

The result of qualitative phytochemistry is presented in Table 2. Generally, 70% ethanol extracted more

Table 3: Total phenolic, total alkaloid, total flavonoid, lycopene, and β-carotene concentration of formulations

	A	B	C	D	E	F	G
TPC (mg GAE/g)	256.88 ± 0.11	278.11 ± 4.34	285.08 ± 1.34	287.14 ± 2.34	290.45 ± 3.77	294.10 ± 2.12	135.8 ± 2.1124[a]
Total alkaloid (mg/g)	181.89 ± 0.34	198.88 ± 0.66	201.34 ± 5.43	215.43 ± 2.22	230.33 ± 1.45	241.34 ± 3.12	128.45 ± 0.99[a]
TFC (mg RE/g)	9.16 ± 0.98	9.05 ± 2.11	9.81 ± 1.01	10.01 ± 0.14	9.78 ± 3.23	10.28 ± 0.92	7.23 ± 0.11[a]
Lycopene (mgCE/g)	0.182 ± 1.25	0.167 ± 0.23	0.131 ± 1.99	0.139 ± 5.77	0.119 ± 0.21	0.071 ± 3.44	0.051 ± 3.44[a]
β-Carotene (mgCE/g)	0.461 ± 0.77	0.379 ± 1.24	0.281 ± 1.09	0.234 ± 2.11	0.159 ± 4.34	0.421 ± 0.907	0.581 ± 0.14[b]

Data are presented as mean ± SD of triplicate determination. [a]Significantly lower than other groups in the same row. [b]Significantly higher than other groups in the same row. A – 100% tomato powder; B – 90% tomato and 10% carrot; C – 80% tomato and 20% carrot; D – 70% tomato and 30% carrot; E – 60% tomato and 40% carrot; F – 50% tomato and 50% carrot; G – 100% carrot. TPC and TFC mean total phenolic content and total flavonoid content, respectively. "mg GAE/g" means mg gallic acid equivalents per gram extracts, "mg RE/g" means mg rutin equivalents per gram extracts, and "mgCE/g mg" means carotenoid equivalents per gram extracts. The total phenolic, flavonoids, and alkaloid concentrations were significantly $p < 0.05$ higher in groups B–F compared to other groups in the study. However, the β-carotene content was higher in Group G (0.581 ± 0.14) compared to other groups in the study.

Table 4: Cytotoxicity assessment of tomato–carrot hydroethanolic extract using the MTT assay

Sample	Concentration (µg/mL)	% Inhibition	IC_{50} (µg/mL)
A	1000	40.28 ±0.08^{a}	
	100	18.43 ± 0.44^{b}	
	10	17.99 ± 0.51^{b}	
	1	11.89 ± 9.71^{bc}	NA
	0.1	9.87 ± 8.77^{bc}	
	0.01	9.77 ± 0.23^{bc}	
	0.001	6.08 ± 8.76^{c}	
	0.0001	3.77 ± 4.56^{c}	
B	1000	30.1 ± 9.99^{q}	NA
	100	13.89 ± 0.65^{b}	
	10	11.56 ± 0.45^{bc}	
	1	9.56 ± 0.44^{bc}	
	0.1	5.88 ± 0.66^{bc}	
	0.01	4.56 ± 0.44^{bc}	
	0.001	3.54 ± 0.34^{c}	
	0.0001	2.56 ± 0.75^{c}	
C	1000	22.1 ± 0.34^{a}	NA
	100	18.89 ± 7.77^{ab}	
	10	10.67 ± 1.02^{bc}	
	1	7.45 ± 0.78^{c}	
	0.1	6.45 ± 0.23^{c}	
	0.01	5.89 ± 0.90^{c}	
	0.001	4.56 ± 2.88^{c}	
	0.0001	3.45 ± 0.99^{c}	
D	1000	19.56 ± 2.45^{a}	NA
	100	13.87 ± 0.02^{b}	
	10	10.45 ± 0.37^{bc}	
	1	8.45 ± 1.11^{cd}	
	0.1	5.79 ± 3.44d^{e}	
	0.01	3.66 ± 2.33^{e}	
	0.001	2.44 ± 0.44^{e}	
	0.0001	1.44 ± 0.45^{e}	
E	1,000	20.3 ± 3.43^{a}	NA
	100	18.45 ± 0.30^{a}	
	10	15.34 ± 0.09^{b}	
	1	14.25 ± 1.99^{b}	
	0.1	11.55 ± 1.21^{c}	
	0.01	9.45 ± 5.45^{c}	
	0.001	5.66 ± 3.45^{d}	
	0.0001	4.67 ± 4.56^{d}	
F	1,000	19.67 ± 4.55a	NA
	100	17.56 ± 3.67^{ab}	
	10	15.43 ± 0.90^{abc}	
	1	13.23 ± 045^{abcd}	
	0.1	10.33 ± 3.22^{bcd}	
	0.01	9.34 ± 4.55^{bcd}	
	0.001	8.56 ± 3.23^{cd}	
	0.0001	5.23 ± 0.67^{d}	
G	1,000	18.96 ± 6.77^{a}	NA
	100	16.45 ± 4.56^{ab}	
	10	14.86 ± 0.52^{abc}	
	1	11.43 ± 2.45^{abc}	
	0.1	10.67 ± 3.44^{abc}	
	0.01	8.67 ± 2.56^{bc}	
	0.001	9.01 ± 3.89^{bc}	
	0.0001	5.33 ± 7.89^{c}	

Data were represented as mean ± SD (n = 3), NA: Not applicable. Mean values that do not share a letter are significantly different.

phytocompounds. Phytocompounds available in the various extracts were terpenoids, cardiac glycosides, saponins, phenols, flavonoids, and alkaloids. Cardiac glycosides are known to have a massive impact on medicine, especially in the treatment and management of several heart conditions. Saponins are chemical compounds found in herbs, seeds, and some vegetables. They are known to have foaming properties, which also boost their antibacterial activity, which has made them very effective in the production of soaps, shampoos, and some household cleaning agents. Biologically, saponins help to reduce cholesterol levels, curb oxidative stress, inhibit tumour growth, and improve lipid metabolism, which aids in the prevention and treatment of obesity [59]. Terpenoids are used in the prophylactic prevention and treatment of certain types of cancers; studies have also shown they possess antifungal, antiparasitic, anti-allergenic, antihyperglycemic, antiviral, and anti-inflammatory properties [60]. Alkaloids are known to contain anaesthetics, cardioprotective, and anti-inflammatory properties [61]. They are very useful in diet formulation and pharmaceuticals for the effective management and treatment of pain [62]. The presence of the phytochemicals gives a useful insight into the therapeutic properties of tomatoes and carrots, as reported by Taiwo et al. [63]. These findings agree with the report of Mariya et al. [64] on the phytochemicals present in tomato and carrot extracts.

6.1.2 Quantitative phytochemical analysis

The result for quantitative phytochemistry of the 70% ethanol extract of the formulations is given in Table 3. The formulations showed a greater number of total phenolics, flavonoids, and alkaloids. For β-carotene and lycopene concentration, the formulation showed a low value. The values reported for β-carotene, lycopene, and phenolics in this study for tomatoes disagree with the report of Bahanla Oboulbiga [65]. Phenolics, flavonoids, lycopene, and β-carotene have been testified to have antioxidant, anticancer, and cardioprotective qualities [66,67]. The highest yield of lycopene was extracted using an improved solvent extraction procedure, yielding a lycopene concentration of 4.34 mg/100 g,

Table 5: Cytotoxicity assessment of lycopene using the MTT assay

Concentration (µg/mL)	% Inhibition	IC_{50} (µg/mL)
1,000	74.2 ± 4.77[a]	149.2
100	29.7 ± 0.33[b]	
10	21.7 ± 0.56[b]	
1	22.2 ± 0.88[bc]	
0.1	29.4 ± 0.77[cd]	
0.01	19.2 ± 0.99[cd]	
0.001	26.0 ± 0.64[d]	

Data were represented as mean ± SD (n = 3). Mean values that do not share a letter are significantly different.

Table 6: Cytotoxicity assessment of camptothecin (standard) extract using the MTT assay

Concentration (µg/mL)	% Inhibition	IC_{50} (µg/mL)
1,000	81.5 ± 0.67[a]	0.44
100	74.2 ± 0.33[b]	
10	74.0 ± 0.45[b]	
1	51.0 ± 0.54[c]	
0.1	29.0 ± 0.01[d]	
0.01	13.3 ± 0.98[e]	

Data were represented as mean ± SD (n = 3). Mean values that do not share a letter are significantly different.

which is lower than the value obtained where [68] acetone:ethylacetate (1:1) was used as the extracting solvent.

6.2 Cytotoxicity assessment

One of the most discussed methods of combating cancer is chemoprevention (Tables 4–6). Apart from lycopene being the major naturally occurring colour pigment in tomatoes, its high antioxidant activity has enhanced its usage in a drastic decrease in the risk of cancer via its epidemiologic and cell culture studies. The anticarcinogenic activity and structure of lycopene have been studied therapeutically on different types of tumour, but its impact on cervical cancer, an asymptomatic condition that causes a high mortality rate in women, is yet to be fully understood. In this study, we evaluated the cytotoxicity effect of tomatoes–carrots mix hydroethanolic extracts lycopene extracted from fresh tomatoes on HeLa cells compared to one of the most frequently used chemotherapeutic drugs in cervical cancer, camptothecin. Figure 1(a) and (b) shows the percentage (%) inhibition graph of the standard drug and the extracted lycopene. Scheme 1 also shows the reduction of 3-(4,5-dimethylthiazol-2-yl)-2,5-diphenyl-2*H*-tetrazolium bromide to 5-(4,5-dimethylthiazol-2-yl)-1,3-diphenyl-formazan. The percentage of cytotoxic inhibition of hydrothanolic extract ranged from 40.28 to 18.96%. Sample A, which is the raw tomato concentrate, shows the highest inhibition concentration of 40.28% with no 50% percentage (%) inhibition. In comparison, the raw carrot concentrate showed a percentage (%) inhibition of 18.96%, which was also the lowest % inhibition. This result indicates that hydroethanolic extracts show no substantial effect on the HeLa cells compared to tomato concentrate. Increasing fortification of the samples with tomatoes slightly increases the cytotoxicity ability of the ethanol extracts. The half-maximal IC_{50} for this extract could not be calculated as there was no 50% cytotoxic inhibition. Sample A recorded the highest % inhibition of 35.21%, while sample E recorded the lowest cytotoxic inhibition of 10.55%.

The highest concentration of lycopene extract (1,000 µg/mL) shows the highest % cytotoxic inhibition of 74.2%, and a drastic decrease was recorded as concentration also decreased. The half minimal IC_{50} of 149.2 µg/mL was calculated using Graph pad Prism 6. Visible massive cell destruction was recorded for the camptothecin-treated cells, as shown in Table 6. The first three concentrations of standard drug-treated cells showed a high percentage (%) of cytotoxic inhibition, which ranged between 81.5 and 74% with IC_{50} of 0.44 µg/mL.

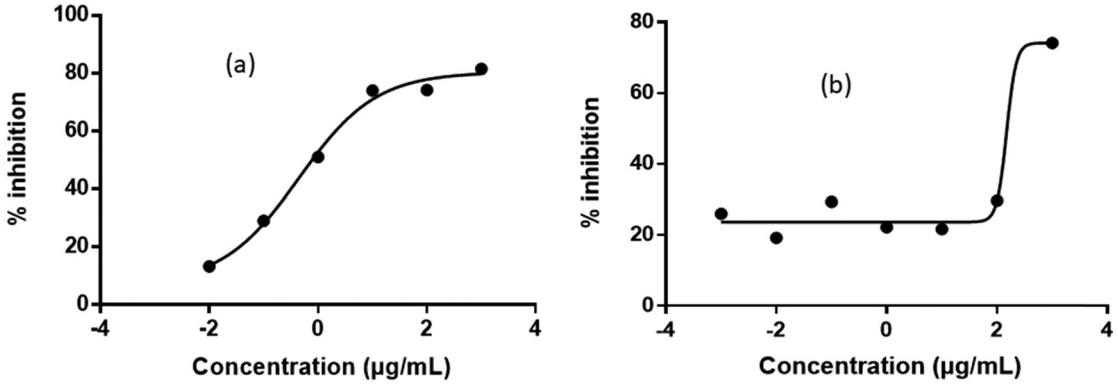

Figure 1: Graph of % inhibition against concentration of camptothecin (a) and lycopene (b).

This result is in accord with the results of Mirahmadi et al. [69], which buttressed the fact that lycopene induces cell arrest that potentiates the antiproliferative mechanism of lycopene. It has also been shown to influence intercellular gap junction communication, the immunological and hormonal systems, and many metabolic processes. It has also been shown to influence intercellular gap junction communication, the immunological and hormonal systems, and many metabolic processes [70]. It should be noted that, unlike other carotenoids, lycopene is not directly diverted to the vitamin A pathway, which enhances its potency to perform different functions, such as an anticancer agent [71]. However, the study has shown that dietary lycopene primarily originates in the linear, all-trans conformation, while lycopene is available mainly in *cis*-isomers in human tissues [72]. The shorter length of the *cis*-isomer increases its absorbing capacity more than its *trans*-isomer; this is due to the greater solubility capacity of the *cis*-isomer in mixed micelles and the lesser propensity of *cis*-isomers to aggregate. The *cis*-isomer is mostly found in the tissue of humans. Consuming lycopene in tomatoes will further enhance its bioavailability in the body system, boosting its anticancer properties.

6.3 Spectroscopic data and structure elucidation of lycopene extract from tomatoes

6.3.1 ^{1}H and ^{13}C NMR

Figure 2a and b shows the ^{1}H and ^{13}C NMR spectrum of the extracted lycopene.

^{1}H NMR chemical shift of the extract was between 0.96 and 4.55 ppm, indicating the absence of any aromatic proton. At 1.0819 ppm, a triplet splitting was identified with a coupling constant of 7.14 Hz, which indicates the presence of methylene (–CH_2). A very high doublet peak was identified at 1.9914 ppm with a coupling constant of 7.87 Hz; the doublet splitting pattern shows the presence of a tertiary carbon, methine (–CH). The high peaks show the presence of several methine groups that are chemically equivalent. A quartet was observed at a chemical shift of 4.0081 ppm with a coupling constant of 7.14 Hz; this indicates the presence of a methyl group (–CH_3).

^{13}C NMR ($CDCl_3$) chemical shift for carbon was from 13.466 to 170.1748 ppm. Carbon shows the presence of seven different carbons with high peaks, indicating chemical equivalence of the carbons. The presence of carbon atoms at 13.466–79.4186 ppm confirms the presence of primary, secondary, and tertiary carbons. All the carbon atoms were identical to the NIST library and published articles [73].

6.3.2 FT-IR analysis

The FT-IR spectrum of lycopene is shown in Figure 3. The bands greater than 3,000 cm^{-1} for the =C–H stretch and the bands that are lower than 3,000 cm^{-1} for the –C–H stretch (alkanes). A C=C stretch band was observed at 1665.74 cm^{-1}. This spectrum also shows the bands for C–H scissoring (1,492 cm^{-1}) and methyl rock (1,435 cm^{-1}), but in general IR analysis, these bands are not only specific to alkenes; also, they are not noted but can be found in most organic molecules in the fingerprint region.

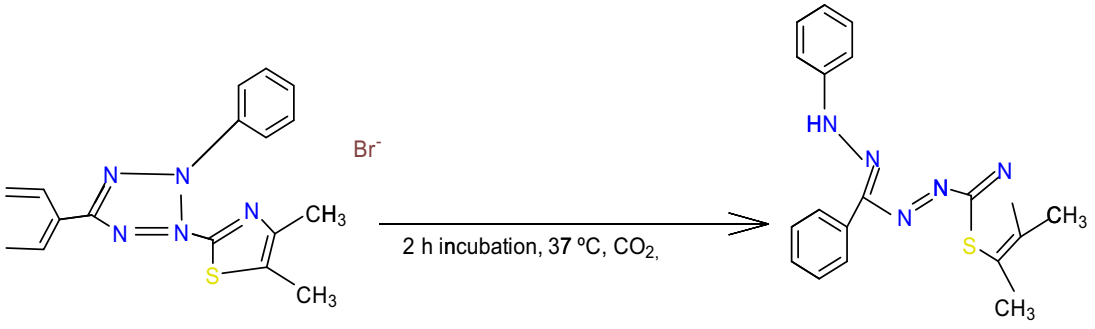

3-(4,5-Dimethylthiazol-2-yl)-2,5-diphenyl-2H-tetrazolium bromide **(MTT)**

(E,Z)-5-(4,5-dimethylthiazol-2-yl)-1,3-diphenyl-formazan (**Formazan**)

Scheme 1: Reduction of MTT reagent.

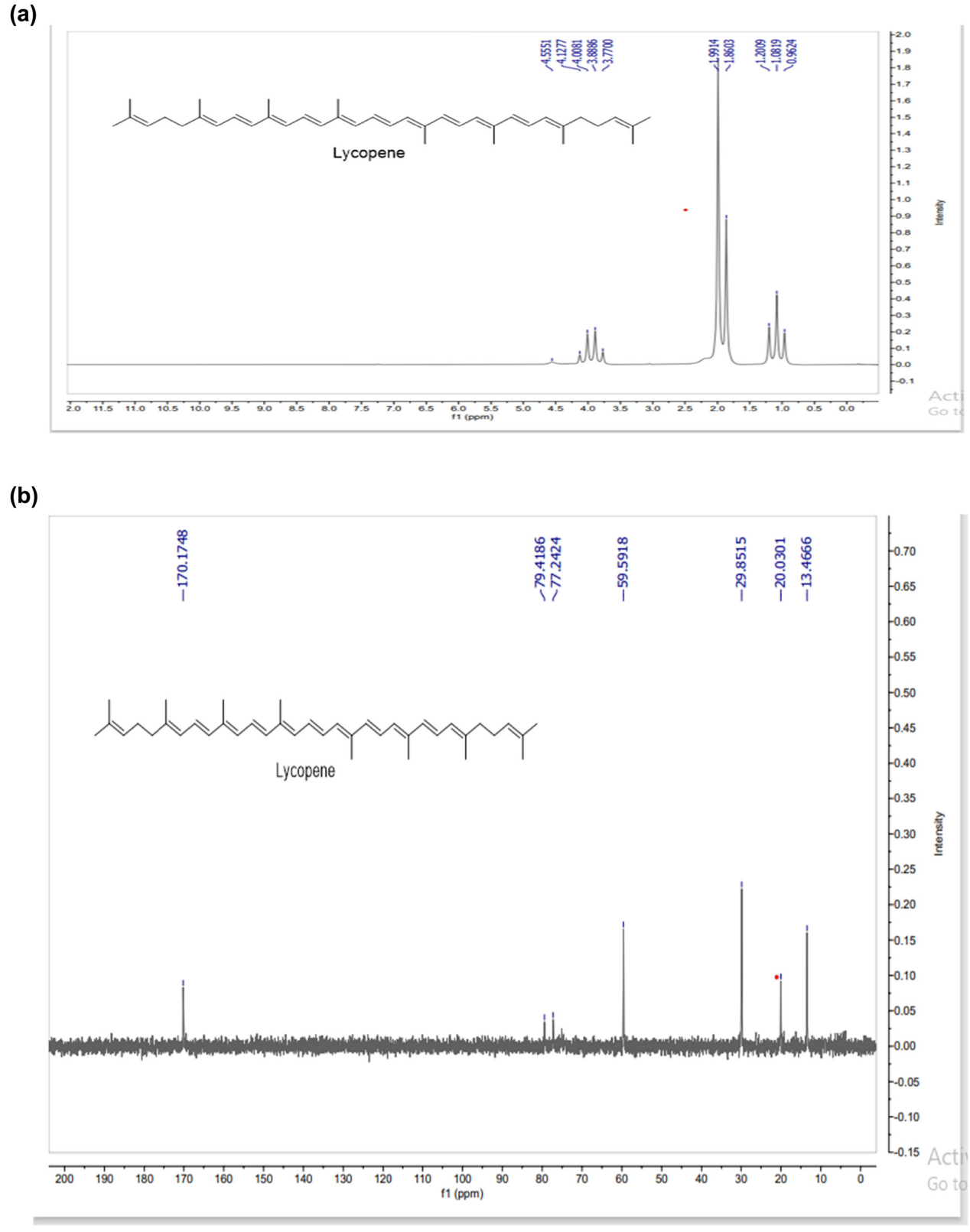

Figure 2: (a) ^{1}H NMR spectrum (60 Hz, $CDCl_2$) of lycopene. (b) ^{13}C NMR spectrum (15 Hz, $CDCl_2$) of lycopene.

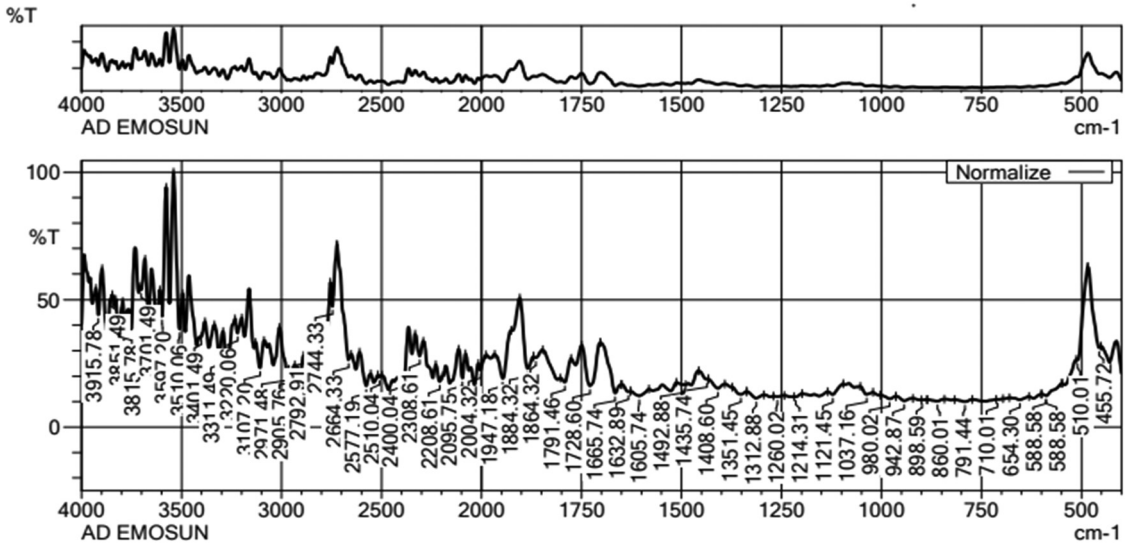

Figure 3: FT-IR spectrum of lycopene.

6.3.3 GC-MS analysis

Figure 4 shows the GC-MS analysis of the extracted lycopene. The mass spectrum chromatography assay showed that the major constituents of lycopene extract included substituted aromatic hydrocarbon, fatty acid primary amide, and long-chain polyene organic compounds. Overall, the most prevalent compounds found in the lycopene extract are 9-octadecenamide (*Z*)-, 1-nonadecene, 9-octadecene, (*E*)-, 1-tetradecene, 1-dodecene, and phenol-3, 4-dimethyl-acetate which accounted for about 80% of the lycopene composition. Among the polyene metabolites, 9-octadecenamide (*Z*)-, 1-nonadecene, and 9-octadecene, *(E)*- were contained in high concentrations, as shown in Table 7. 1-Nonadecene was the predominant organic compound, an unsaturated polyene structure, a nitrogen-containing compound found in plants, and also exhibits excellent anti-inflammatory properties.

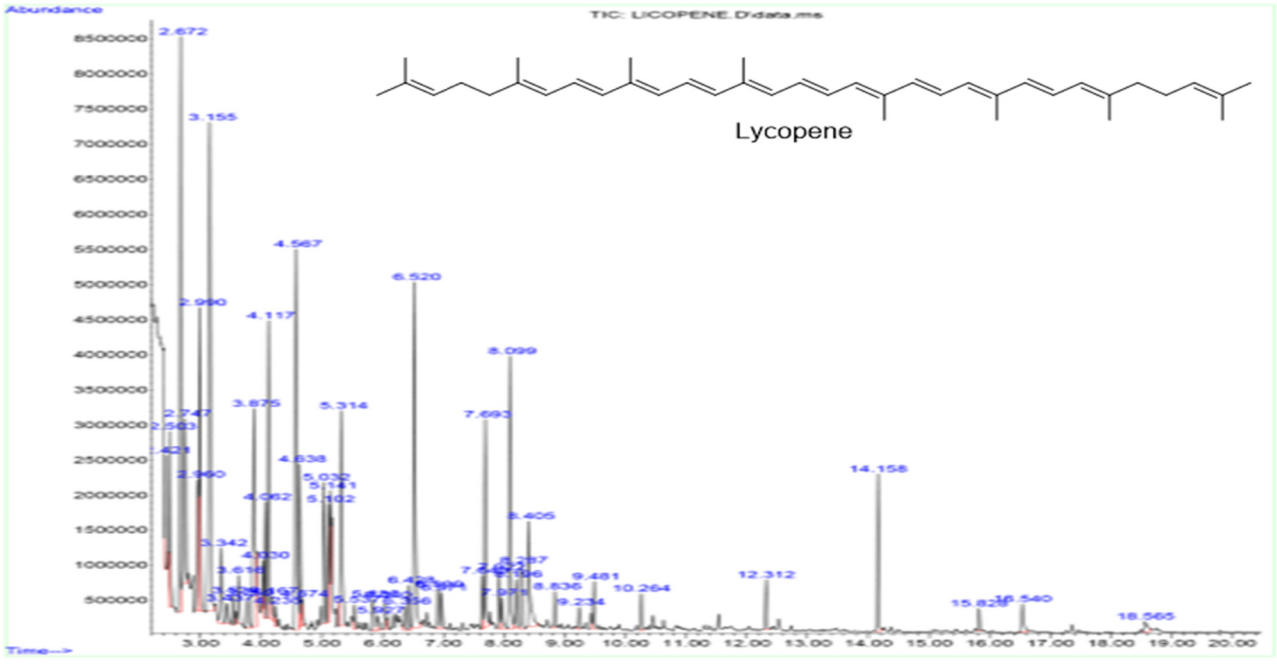

Figure 4: GC-MS chromatogram of lycopene.

Table 7: Compounds identified in the lycopene extract by GC-MS

Sample no	Retention time	% Composition	Library ID	Molecular formula (molecular weight)
1	16.54	4.3714	9-Octadecenamide, (*Z*)-	$C_{18}H_{35}NO$, 281.272
2	14.148	4.1386	1-Nonadecene	$C_{19}H_{38}$, 266.5
3	10.264	3.9208	9-Octadecene, (*E*)-	$C_{18}H_{36}$, 252.5
4	9.481	3.0495	1-Tetradecene	$C_{14}H_{28}$, 196.37
5	7.922	2.6139	1-Dodecene	$C_{12}H_{24}$, 168.32
6	8.405	2.5501	Phenol-3,4-dimethyl-acetate	$C_{10}H_{12}O_2$, 122.16
7	9.234	2.4882	2,5,6-Trimethylbenzimidazole	$C_9H_{11}N_3$, 161.20
8	8.836	2.2208	Naphthalene, 1-methyl-	$C_{14}H_{16}$, 188.28
9	8.099	2.2703	1*H*-Benzimidazole, 5,6-dimethyl-	$C_9H_{10}N_2$, 146.19
10	6.52	2.0523	Benzofuran, 7-methyl-	$C_9H_8O_2$, 132.16.

6.4 In silico analysis

6.4.1 Molecular docking analysis

The binding affinity for the lycopene-treated HeLa cells after docking with anti-apoptotic human BCL-2 protein (IG5M) and pro-apoptotic (agonist) BAX 1 protein (4S0O) was used to measure its inducement of apoptosis. The inhibitory effect caused by the interaction of the ligands with the anti-apoptotic protein or the activation of the pro-apoptotic protein to heighten apoptosis will guide further investigations in this field of study. The activity of the lycopene ligand is measured by its tendency to fit properly into the protein cavity of the receptor and also considerably bind with amino acids in the presence of the active site.

The binding energy, bond distance, and 2D visualization of amino acid residues of pro-apoptotic BAX 1 protein (4S0O) with lycopene ligand with reference to camptothecin (standard drug) are displayed in Table 8 and Figure 5(a) and (b). The lowest binding affinity of −8.8 kcal mol^{-1} was recorded for the standard drug, while −5.6 kcal mol^{-1} was documented for lycopene. Camptothecin showed hydrogen bond interaction with Glu-41, Leu-47, and Glu-32, but this H bond interaction was not exhibited by the lycopene ligand but positive alkyl interactions with Ala-97, Arg-147, Phe-93, Trp-170, Arg: 65, Leu: 162, Cys: 62 was visible in the three-dimensional visualization of the lycopene ligand docking. The active and highest binding affinity for the standard drugs was recorded between C7 and C16 of the ligand structure, which indicates a good interaction with the pro-apoptotic protein (4S0O). The camptothecin ligand indicated a much greater advantage over lycopene since there are more H bond interactions with the human pro-apoptotic protein. The low bond distance between the H bond interactions Glu: 2.3 of the ligands and the protein also indicates a very strong binding affinity, which is a good reference for a potential active drug. The alkyl and pi–alkyl interactions of the lycopene ligand with the pro-apoptotic HeLa protein will not produce a strong effect as compared to the standard drug. Therefore, the camptothecin ligand with higher binding affinity, short bond distance, and strong hydrogen bonding affinity is considered a downregulation via an intrinsic mechanism that promotes HeLa cancer cell apoptosis.

The binding energy, bond distance, and 2D visualization of amino acid residues of anti-apoptotic BCL-1 protein (1G5M) with lycopene ligand with reference to camptothecin (standard drug) are shown in Table 9 and Figure 5(c) and (d). The highest hydrogen bond binding affinity of −2.6 kcal mol^{-1} was recorded for the standard drug as a result of interaction with His-20 amino acid residue and a short

Table 8: Binding energy and bond distance of lycopene and camptothecin with pro-apoptotic BAX I protein (4S0O)

Ligands binding affinity (kcal mol^{-1})	Amino acid residue	Bond distance
Lycopene −5.6 kcal mol^{-1}	**Alkyl interactions**: **ALA**-97, **ARG**-147, **PHE**-93 **Pi–alkyl interactions:** **TRP**-170, **ARG**:65, **LEU**: 162, **CYS**: 62	**ALA**: 4.92, **ARG**: 5.07, **PHE**: 4.49, **TRP**:4.90, **ARG**: 4.00, 4.49, **LEU**: 4.97, **CYS**: 4.04
Camptothecin −8.8 kcal mol^{-1}	**Conventional hydrogen bond**: **GLU**:41, **Carbon Hydrogen bond:** **LEU**: 47, **Pi–donor hydrogen bond**: **GLN**:32, **Pi–sigma bond**: **ALA**:46, **ILE**: 133, **Pi–Alkyl**: **LEU**:45, **ARG**: 134	GLU: 2.3, LEU: 4.94, GLN: 3.58, ALA: 3.79, 4.79, ILE: 3.82, 5.22,ARG: 5.22, LEU: 5.20

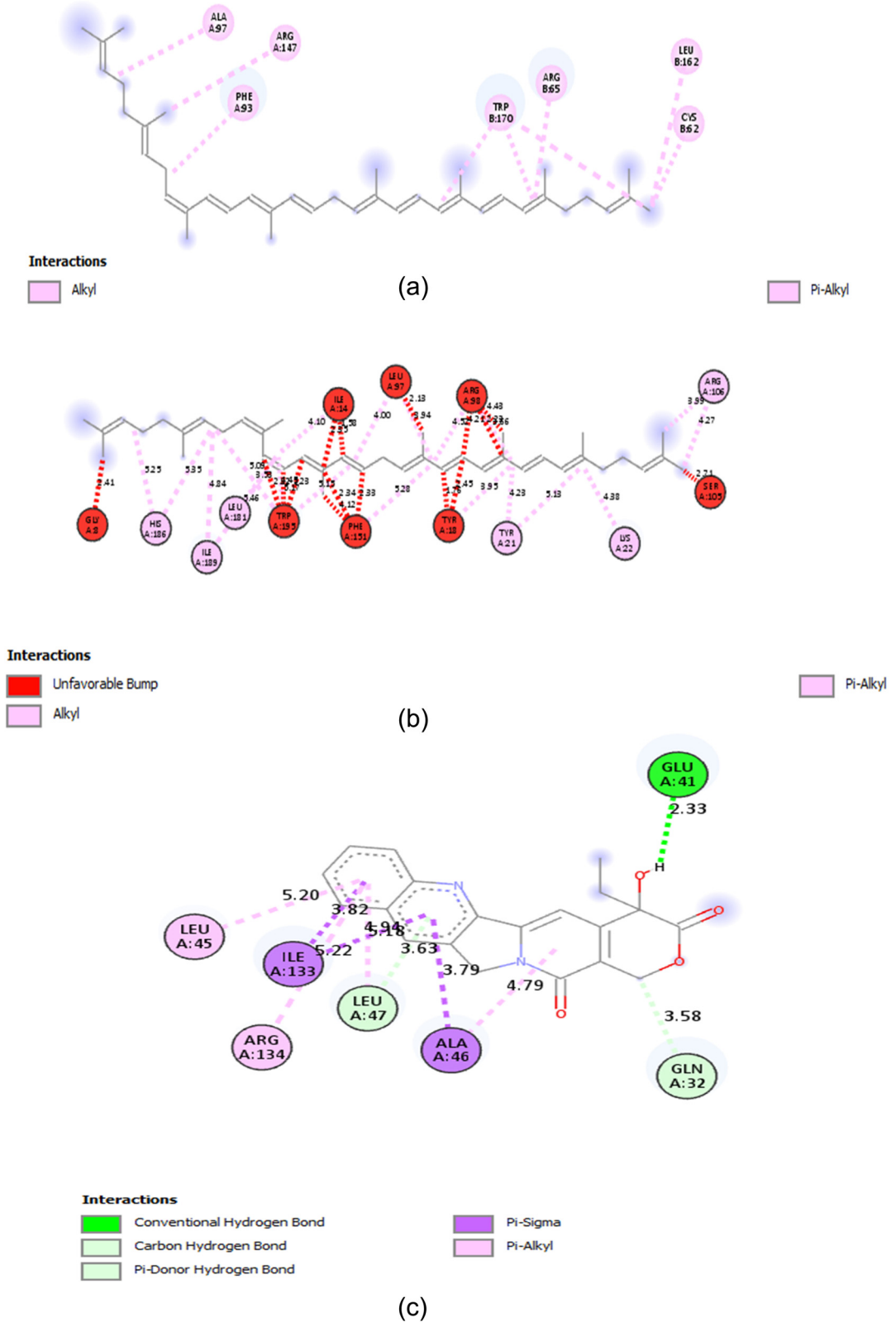

Figure 5: (a) 2D representation of lycopene with pro-apoptotic BAX I protein (4S0O) indicating the amino acid residues, (b) 2D representation of lycopene with anti-apoptotic HUMAN BCL-2 protein (IG5M) indicating the amino acid residues, (c) 2D representation of Camptothecin with pro-apoptotic BAX I protein (4S0O) indicating the amino acid residues, and (d) 2D representation of camptothecin with anti-apoptotic HUMAN BCL-2 protein (IG5M) indicating the amino acid residues.

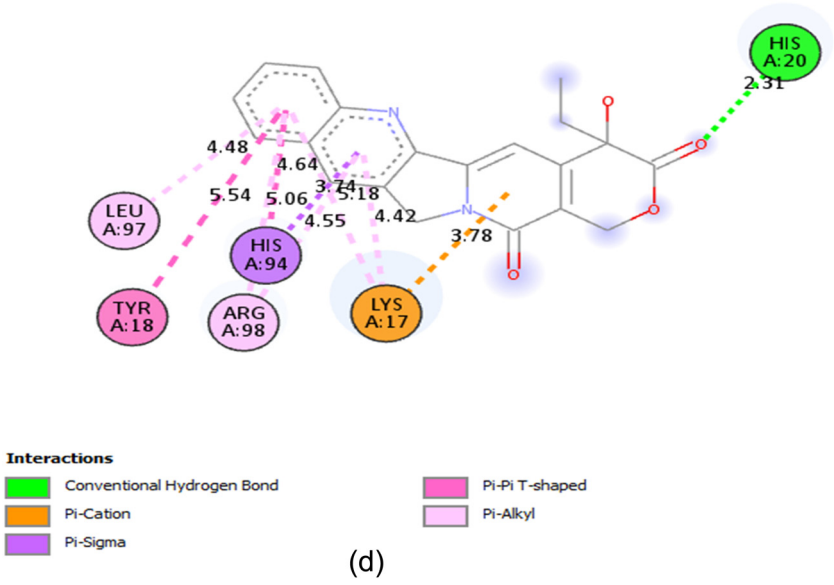

(d)

Figure 5: (*Continued*)

bond distance of His-2.31 with positive Pi–cation interaction due to Lys-17 amino acid residue, Pi–sigma interaction due to His-94 amino acid residue, Pi–Pi T-shaped interaction due to Tyr-18 amino acid residue and Pi–alkyl interaction due to Leu-97 and Arg-98 amino acid residues. Lycopene ligand showed favourable alkyl bond interaction due to His-186, Ile-189, and Leu-181 amino acid residues and Pi–alkyl bond interactions due to Tyr-21, Lys: 22, and Arg: 106 amino acid residues with a low binding affinity of 39.6 kcal mol^{-1}.

This result indicates that lycopene ligand promotes cervical cancer apoptosis using human cell lines (HeLa cell lines) from the anti- and pro-apoptotic protein interactions, but further functionalization of the lycopene ligand will enhance its usage as an effective cervical cancer prophylactic drug.

6.4.2 MD simulation analysis

To validate the stability of the lycopene binding mode, MD simulations are performed. We executed a 100 ns MD simulation of lycopene in complex with proteins 1G5M and 4S0O to investigate their structural study and ensure steady binding under dynamic conditions. The study of root mean square deviation (RMSD) is a numerical formula that measures the average change in displacement of a group of atoms with respect to a reference (initial) frame, demonstrating the structural stability of the protein–ligand complex. The degree of variance in RMSD is inversely related to complex stability: the lesser the variation, the more stable the complex [57,74]. The average Cα RMSD values for the lycopene–1G5M and lycopene–4S0O complexes were

Table 9: Binding energy and bond distance of lycopene and camptotechin with isoform 1 of anti-apoptotic human BCL-2 protein (IG5M)

Ligands binding affinity (kcal/mol)	Amino acid residue	Bond distance
Lycopene 39.6 kcal/mol	**Unfavourable bump**: **GLY**-8, **ILE**-14, **LEU**-97, **ARG**-98, **TYR**-18, **PHE**-151, **TRP**-195, **SER**-105, **Alkyl Bond**: **HIS**-186, **ILE**-189, **LEU**-181, **Pi-alkyl Bond**: **TYR**-21, **LYS**: 22, **ARG**: 106	**GLY**-2.41, **ILE**-1.58,2.35 **LEU**-2.31, 3.94 **ARG**-4.52, 2.12 **TYR**-1.76, 2.45, **PHE**-4.12, 2.34, 2.33, **TRP**-5.71, 2.42, **SER**-2.71, **HIS**-5.25,5.35 **ILE**-4.84, **LEU**-5.46, **TYR**-4.23, 5.13, **LYS**: 4.38, **ARG**: 3.99, 4.27
Camptothecin −2.6 kcal/mol	**Conventional hydrogen bond**: **HIS**-20, **Pi–cation**-**LYS**-17, **Pi–Sigma**-**HIS**-94, **Pi–Pi T-Shaped**; **TYR**-18, **Pi–Alkyl**: **LEU**-97, **ARG**-98	**HIS**-2.31, **LYS**-3.78, -**HIS**-4.64, 3.74, **ARG**-5.06, 4.55,**TYR**:5.54, **LEU**-4.48

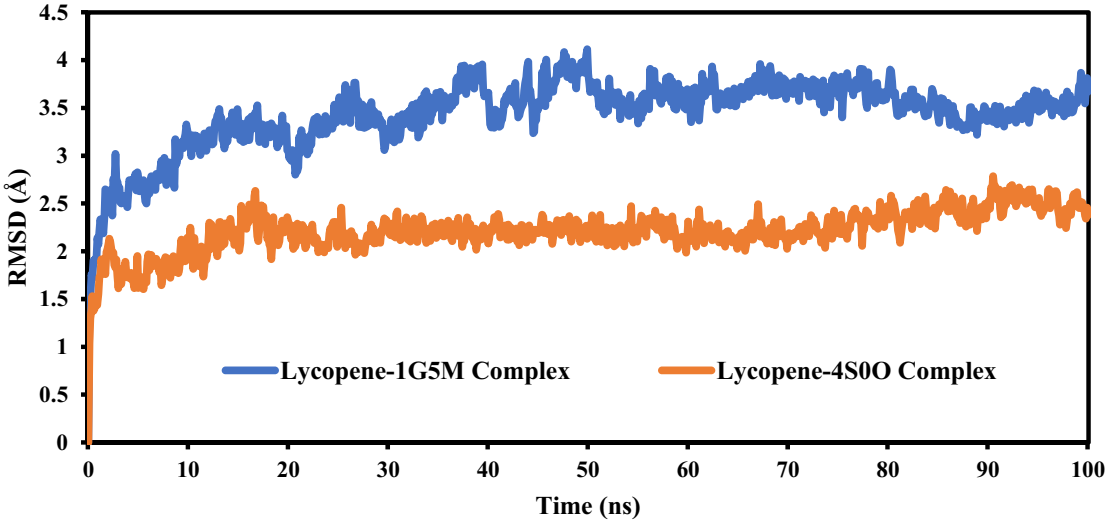

(a)

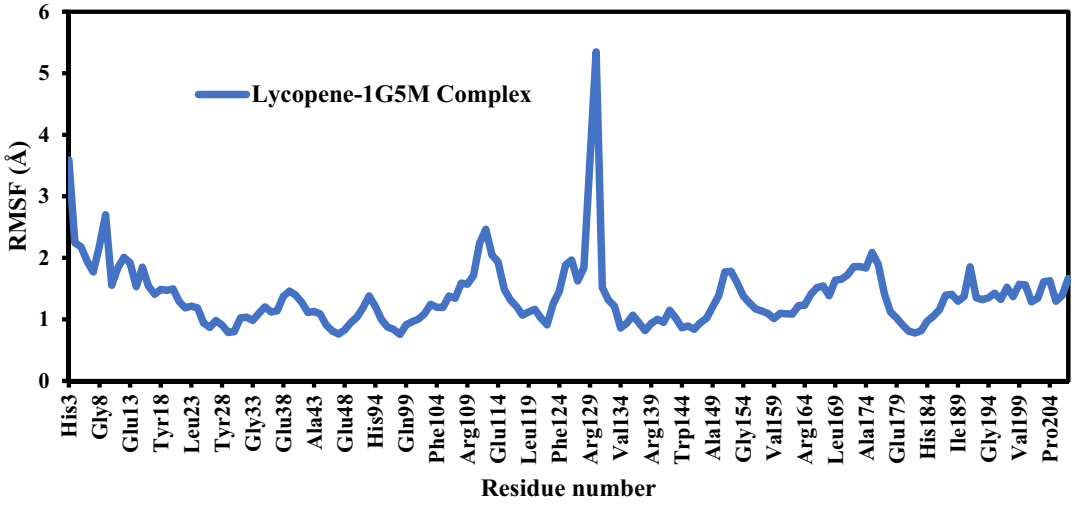

(b)

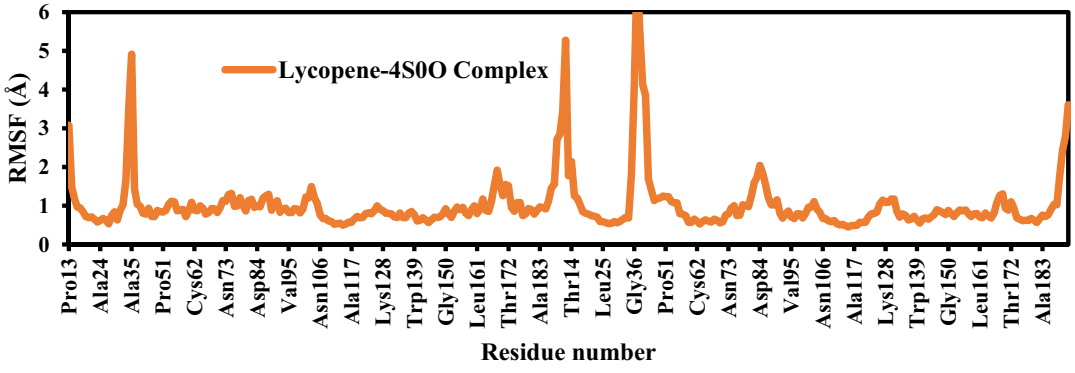

(c)

Figure 6: (a) MD simulation analysis of lycopene–1G5M complex (blue) and lycopene–4S0O complex (red). (b) Time-dependent protein Cα atoms RMSD for lycopene–IG5M complex. (c) Protein individual amino acid RMSF of lycopene–1G5M complex. (d) Radius of gyration analysis data for lycopene (IG5M, 4S0O) complexes obtained from MD trajectory. (e) Radius of gyration analysis data derived from the MD trajectory.

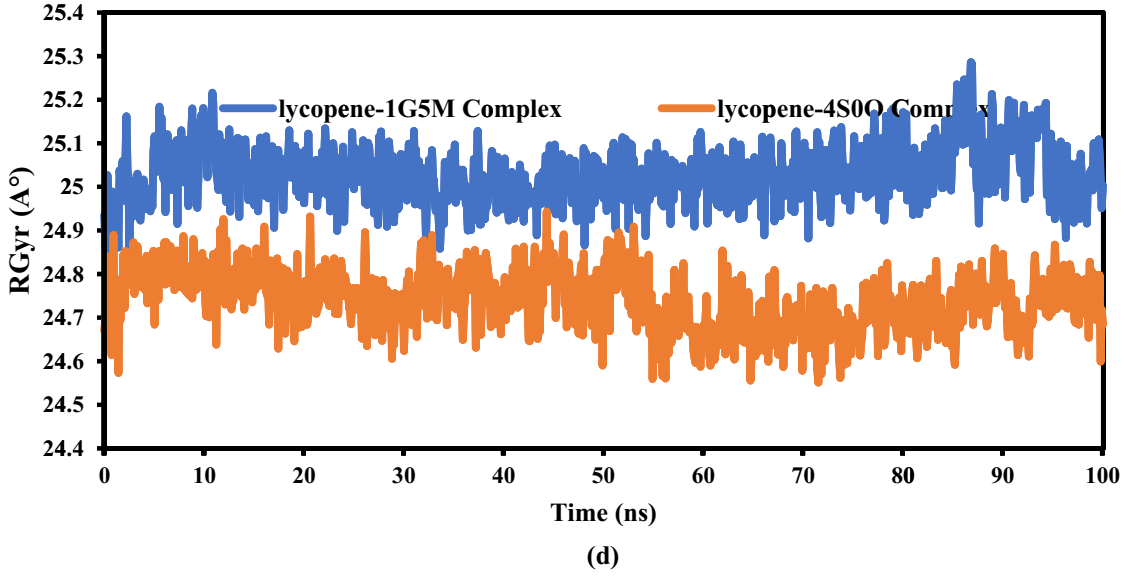

(d)

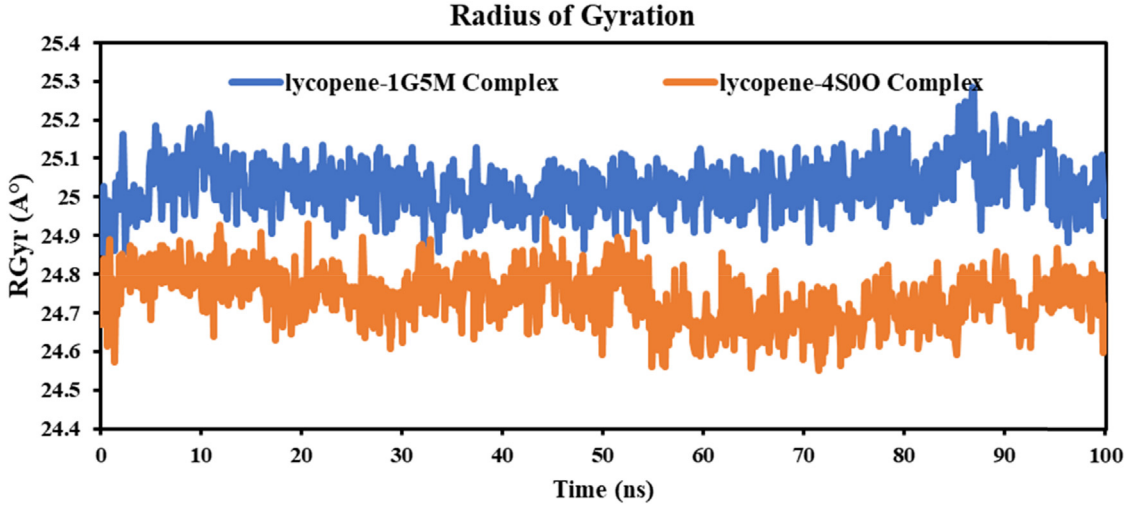

(e)

Figure 6: (*Continued*)

3.439 ± 0.37 and 2.211 ± 0.22 Å, respectively. The RMSD in the lycopene–1G5M complex remained in the range of 1.72–4.07 Å after initial fluctuation due to equilibration until 48 ns; after that, minor fluctuation was observed until the end of the simulation. On the other hand, the RMSD of the lycopene–4S0O complex has been consistent throughout the simulation time, with a maximum fluctuation of 2.7 Å (Figure 6(a)). The RMSD of both complexes was minimal compared to their beginning coordinates, indicating that the complexes remained stable during the simulation.

The RMSF was computed to analyse the residual fluctuations over the simulation time. High RMSF peaks (values) showed the existence of terminal ends, loops, twists, and loose bonding, indicating the protein structure's flexibility, while lower values showed the presence of secondary structures such as β-sheets and α-helices, indicating the structure's stability [75,76]. The lycopene–1G5M complex shows higher fluctuation from residual index Gly128 to Ala131, which is positioned in the loop region and is not engaged in ligand binding. In this complex, lycopene interacted with 18 amino acids of 1G5M protein, including Tyr9 (1.1 Å), Ile14 (0.8 Å), Val15 (0.8 Å), Tyr18 (0.8 Å), Val93 (0.7 Å), Leu97 (0.6 Å), Phe104 (0.9 Å), Ala113 (0.7 Å), Ile147 (0.6 Å), Val148 (0.5 Å), Ala149 (0.5 Å), Phe151 (0.5 Å), Leu175 (0.8 Å), Met177 (0.8 Å), Leu181 (0.9 Å), Ile189 (0.7 Å), Trp195 (0.9 Å), and Phe198 (1.0 Å) (Figure 6(b)). On the other hand, ten amino acids of 4S0O protein make contact with lycopene namely, Phe92 (0.8 Å), Phe93 (0.9 Å), Ala96 (0.8 Å), Ala97 (0.9 Å), Phe100

(0.9 Å), Trp139 (0.8 Å), Phe143 (0.6 Å), Cys62 (0.6 Å), Leu162 (0.7 Å), and Trp170 (0.9 Å). High fluctuation is observed in this complex with residues Gly36 (4.0 Å), Pro43 (4.1 Å), Ala35 (4.9 Å), Gly192 (5.2 Å), Ala42 (5.4 Å), and Glu41 (7.1 Å), which are located away from the lycopene binding site (Figure 6(c)). The residues in the pocket create the active site for lycopene binding had a low RMSF between 1 and 2 Å, owing to its structural confirmation.

The radius of gyration (RGyr) was calculated to determine the structure's compactness. RGyr of a stably folded protein remains relatively constant across the simulation duration [77]. The time-dependence plot of the RGyr for the simulated lycopene–1G5M and lycopene–4S0O complexes is shown in Figure 6(d). As can be observed, the RGyr values did not change significantly, and the compactness was sustained throughout the 100 ns trajectory. The RGyr values ranged from 24.57 to 25.11 Å. The average RGyr values of the lycopene–1G5M and lycopene–4S0O complexes were 25.03 and 24.74 Å, respectively, in Figure 6(e). The lower value of RGyr implies that the protein–ligand complex is smaller. According to the overall quality study performed by RMSD and RGyr, lycopene considerably contributes to the stability by efficiently binding to the target 1G5M and 4S0O proteins in the binding cavity.

The MM-GBSA method was employed to assess the binding free energy of the lycopene–protein complexes. This was accomplished by utilizing trajectory frames derived from MD simulations. In contrast to conventional molecular docking, this approach takes into consideration the dynamic interactions between the protein and ligands, resulting in more precise binding free energy calculations. For the binding free energy calculation, the last 10 ns snapshot was utilized. The average binding free energy (Δ*G* bind) provides an estimation of the overall binding affinity for each inhibitor. Elevated average values indicate robust binding interactions, while lower values imply weaker interactions. The calculated ΔG bind values for the lycopene–IG5M and lycopene–4S0O complexes reveal intriguing differences in their binding affinities. In the case of the lycopene–4S0O complex, it exhibits a notably higher maximal free binding energy (−83.81 kcal mol^{-1}) in comparison to lycopene–IG5M complex (−80.45 kcal mol^{-1}). This suggests that the lycopene–4S0O complex forms more stable binding interactions with its target, potentially indicating a higher affinity. Conversely, the lycopene–IG5M complex shows a wider range of binding energies, with a lower minimum (Δ*G* bind of −44.05 kcal mol^{-1}) compared to the lycopene–4S0O complex's minimum (Δ*G* bind of −30.42 kcal mol^{-1}), indicating that the lycopene–IG5M complex experiences weaker binding interactions at its lowest energy state. On average, the lycopene–4S0O complex demonstrates a stronger binding affinity (−78.65 kcal mol^{-1}) than the lycopene–IG5M complex (−72.71 kcal mol^{-1}). The standard deviation values, which are similar for both complexes, suggest that the binding energies within each complex exhibit comparable levels of variability. These Δ*G* bind results provide valuable insights into the relative binding strengths of these two complexes, offering a foundation for further investigations into their interactions and potential implications for drug design or therapeutic applications.

7 Conclusion

This study has shown that fortification of tomato concentrates with carrot concentrate significantly increased the flavonoid, phenolic, lycopene, and β-carotene content of the tomatoes. The ^{1}H and ^{13}C NMR analysis of the extracted lycopene confirms the structure of lycopene ($C_{50}H_{46}$), while the FT-IR further revealed the presence of conjugation at 3,000 and 1,665.74 cm^{-1}. GC-MS analysis showed the presence of some substituted aromatic hydrocarbons and long-chain polyene organic compounds. Extracted lycopene from tomato showed more promising anticancer activity than the tomato–carrot food mix, which was made evident in its interactions with pro-apoptotic and anti-apoptotic ligands of the HeLa cell proteins; also, the cytotoxic assessment of tomato–carrot food mix is a novel research which is an added advantage to knowledge. The *in silico* evaluation proves that lycopene extracted from *S. lycoperscicum* promotes cell apoptosis in cervical cancer cells than the hydroethanolic extract of tomato–carrot food mix.

Acknowledgments: The authors would like to appreciate the management of Covenant University in Ota, Ogun State, and the Nigerian Institute of Medical Research (NIMR) in Yaba, Lagos State, for providing research funding and cutting-edge laboratory equipment.

Funding information: The research was financially supported by Covenant University in Ota, Nigeria.

Author contributions: Methodology and writing – original manuscript; O.T. Ademosun. Project validation; O.T. Ademosun; A.H. Adebayo; K.O.Ajanaku. Investigation; O.T. Ademosun; E.C. Agwamba, I.Ahmad; H.Patel; H. Louis. Formal Analysis: E.C. Agwamba, I.Ahmad; H.Patel; H. Louis. Reviewing; O.T. Ademosun; E.C. Agwamba. Supervision: A.H. Adebayo; K.O.Ajanaku All the authors agreed on the final version of the manuscript.

Conflict of interest: The authors have no conflicts of interest to declare.

Ethical approval: The conducted research is not related to either human or animals use.

Data availability statement: All the data created or analysed during this research is contained in this published article and its supporting material files.

References

[1] de Martel C, Georges D, Bray F, Ferlay J, Clifford GM. Global burden of cancer attributable to infections in 2018: A worldwide incidence analysis. Lancet Glob Health. 2020;8(2):e180–90.

[2] World Health Organization. Global Reference List of 100 Core Health Indicators (plus health-related SDGs) 2018; 2018; p. 164.

[3] American Cancer Society. American Cancer Society: Cancer Facts & Figures 2014. Cancer Facts and Figures; 2014.

[4] Kuiava VA, Chielle EO. Epidemiology of cervix cancer in Brazil (2005–2015): study of mortality and hospital intervention rates. Arch Biosci Health. 2019 Jun;1(1):45–60.

[5] Bosch FX, De Sanjosé S. The epidemiology of human papillomavirus infection and cervical cancer. Dis Markers; 2007;23:213–27.

[6] Momenimovahed Z, Salehiniya H. Delay in the diagnosis of breast cancer during coronavirus pandemic. EXCLI J. 2021;20:142–4.

[7] Tomita LY, Horta BL, da Silva LLS, Malta MB, Franco EL, Cardoso MA. Fruits and vegetables and cervical cancer: A systematic review and meta-analysis. Nutr Cancer. 2021;73(1):62–74. doi: 10.1080/01635581.2020.1737151.

[8] Lacey JV, Swanson CA, Brinton LA, Altekruse SF, Barnes WA, Gravitt PE, et al. Obesity as a potential risk factor for adenocarcinomas and squamous cell carcinomas of the uterine cervix. Cancer 2003 Aug;98(4):814–21.

[9] Organization WH. WHO Report on Surveillance of Antibiotic Consumption; 2018. p. 113.

[10] Kane MA, Serrano B, De Sanjosé S, Wittet S. Implementation of human papillomavirus immunization in the: Developing world. Vaccine 2012; 30(Suppl.5):F192–200.

[11] Lim CB, Ky N, Ng HM, Hamza MS, Zhao Y. Curcuma wenyujin extract induces apoptosis and inhibits proliferation of human cervical cancer cells *in vitro* and *in vivo*. Integr Cancer Ther. 2010 Mar;9(1):36–49.

[12] Gali-Muhtasib H, Roessner A, Schneider-Stock R. Thymoquinone: A promising anti-cancer drug from natural sources. Int J Biochem Cell Biol. 2006;38:1249–53.

[13] Kishore RK, Halim AS, Syazana MSN, Sirajudeen KNS. Tualang honey has higher phenolic content and greater radical scavenging activity compared with other honey sources. Nutr Res. 2011 Apr; 31(4):322–5.

[14] Zhang Z, Knobloch TJ, Seamon LG, Stoner GD, Cohn DE, Paskett ED, et al. A black raspberry extract inhibits proliferation and regulates apoptosis in cervical cancer cells. Gynecol Oncol. 2011 Nov;123(2):401–6.

[15] Vanathi P, Narendhran S, Rajiv P, Sivaraj R. Spectroscopic analysis of bioactive compounds from *Streptomyces cavouresis* kuv39: Evaluation of antioxidant and cytotoxicity activity. Int J Pharm Pharm Sci. 2014;6:319–22. https://www.researchgate.net/publication/267035742.

[16] Santos PASR, Avanço GB, Nerilo SB, Marcelino RIA, Janeiro V, Valadares MC, et al. Assessment of cytotoxic activity of rosemary (*Rosmarinus officinalis* L.), turmeric (*Curcuma longa* L.), and ginger (*Zingiber officinale* R.) essential oils in cervical cancer cells (HeLa). Sci World J. 2016;1–10.

[17] Gong G, Liu Q, Deng Y, Dang T, Dai W, Liu T, et al. Arabinogalactan derived from Lycium barbarum fruit inhibits cancer cell growth via cell cycle arrest and apoptosis. Int J Biol Macromol. 2020;149:639–650. https://www.sciencedirect.com/science/article/pii/S0141813019371223.

[18] Alvarez-Sala A, Attanzio A, Tesoriere L, Garcia-Llatas G, Barberá R, Cilla A. Apoptotic effect of a phytosterol-ingredient and its main phytosterol (β-sitosterol) in human cancer cell lines. Int J Food Sci Nutr. 2019;70(3):18–24. doi: 10.1080/09637486.2018.1511689.

[19] Luo J, Meng X, Su J, Ma H, Wang W, Fang L, et al. Biotin-modified polylactic-*co*-glycolic acid nanoparticles with improved antiproliferative activity of 15,16-dihydrotanshinone I in human cervical cancer cells. J Agric Food Chem. 2018 Sep;66(35):9219–30. doi: 10.1021/acs.jafc.8b02698.

[20] Larbat R, Paris C, Le Bot J, Adamowicz S. Phenolic characterization and variability in leaves, stems and roots of Micro-Tom and patio tomatoes, in response to nitrogen limitation. Plant Sci. 2014;224:62–73.

[21] Ademosun OT, Adebayo AH, Ajanaku KO. Solanum lycopersicum and *Daucus carota*: effective anticancer agents a mini review. J Phys Conf Ser. 2021 Jul;1943(1):12169. doi: 10.1088/1742-6596/1943/1/012169.

[22] Perveen R, Suleria HAR, Anjum FM, Butt MS, Pasha I, Ahmad S. Tomato (Solanum lycopersicum) carotenoids and lycopenes chemistry; metabolism, absorption, nutrition, and allied health claims – A comprehensive review. Crit Rev Food Sci Nutr. 2015 Jun;55(7):919–29.

[23] Ademosun OT, Ajanaku KO, Adebayo AH, Oloyede MO, Okere DU, Akinsiku AA, et al. Physico-chemical, microbial and organoleptic properties of yoghurt fortified with Tomato Juice. J Food Nutr Res. 2019;7:810–4. https://api.semanticscholar.org/CorpusID:214506983.

[24] Campestrini LH, Melo PS, Peres LEP, Calhelha RC, Ferreira ICFR, Alencar SM. A new variety of purple tomato as a rich source of bioactive carotenoids and its potential health benefits. Heliyon 2019;5(11):1–8.

[25] Kuklev D V, Domb AJ, Dembitsky VM. Bioactive acetylenic metabolites. Phytomedicine. 2013;20(13):1145–59. https://www.sciencedirect.com/science/article/pii/S0944711313002158.

[26] Sharoni Y, Danilenko M, Walfisch S, Amir H, Nahum A, Ben-Dor A, et al. Role of gene regulation in the anticancer activity of carotenoids. Pure Appl Chem. 2002;74(8):1469–77.

[27] Perusek L, Maeda T. Vitamin a derivatives as treatment options for retinal degenerative diseases. Nutrients. 2013;5(7):2646–66.

[28] Wang Y, Gallegos JL, Haskell-Ramsay C, Lodge JK. Effects of chronic consumption of specific fruit (berries, citrus and cherries) on CVD risk factors: a systematic review and meta-analysis of randomised controlled trials. Eur J Nutr. 2021;60(2):615–39. doi: 10.1007/s00394-020-02299-w.

[29] Mora-Esteves David CS. Nutrient supplementation: Improving male fertility fourfold. Semin Reprod Med. 2013;31(04):293–300. http://www.thieme-connect.com/products/ejournals/abstract/10.1055/s-0033-1345277.
[30] Trejo-Solís C, Pedraza-Chaverrí J, Torres-Ramos M, Jiménez-Farfán D, Cruz Salgado A, Serrano-García N, et al. Multiple molecular and cellular mechanisms of action of lycopene in cancer inhibition. J Evidence-Based Complementary Altern Med. 2013;1–17.
[31] GE. Tomatoes, Tomato-Based products, lycopene, and cancer: review of the epidemiologic literature; 1999. https://academic.oup.com/jnci/article/91/4/317/2543924.
[32] Ronsein GE, Miyamoto S, Bechara E, Di Mascio P, Martinez GR. Oxidação de proteínas por oxigênio singlete: Mecanismos de dano, estratégias para detecção e implicações biológicas. Quim Nova. 2006;29(3):563–8.
[33] Stahl W, Sies H. Bioactivity and protective effects of natural carotenoids. Biochimica et Biophysica Acta – Mol Basis Dis. 2005;1740(2):101–7.
[34] Gift Nwaokoro O. Effect of the addition of hydrocolloids to tomato-carrot juice blend. J Nutrit Health Food Sci. 2015;3(1):1–10.
[35] Lee HJ, Park YK, Kang MH. The effect of carrot juice, β-carotene supplementation on lymphocyte DNA damage, erythrocyte antioxidant enzymes and plasma lipid profiles in Korean smoker. Nutr Res Pract. 2011;5(6):540–7.
[36] Varshney K, Mishra K. An analysis of health benefits of carrot. Int J Innovative Res Eng & Manag. 2022 Feb;9:211–4.
[37] Tibäck E, Langton M, Oliveira J, Ahrné L. Mathematical modeling of the viscosity of tomato, broccoli and carrot purees under dynamic conditions. J Food Eng. 2014;124:35–42.
[38] Briviba K, Bub A, Roser S, Pool-zobel BL, Rechkemmer G. Effects of carrot and tomato juice consumption on faecal markers relevant to colon carcinogenesis in humans Br J Nutr. 2008;606–13.
[39] Bule M V., Singhal RS. Use of carrot juice and tomato juice as natural precursors for enhanced production of ubiquinone-10 by *Pseudomonas diminuta* NCIM 2865. Food Chem. 2009;116(1):302–5.
[40] Bule M V, Singhal RS. Use of carrot juice and tomato juice as natural precursors for enhanced production of ubiquinone-10 by *Pseudomonas diminuta* NCIM 2865. Food Chem. 2009;116(1):302–305.doi: 10.1016/j.foodchem.2009.02.050.
[41] Pandya D. Standardization of solvent extraction process for lycopene extraction from tomato pomace. J Appl Biotechnol & Bioeng. 2017;2(1):12–6.
[42] Varadharaj V, Varadharajan V, Kumba Janarthanan U, Krishnamurthy V. Physicochemical, phytochemical screening and profiling of secondary metabolites of *Annona squamosa* leaf extract. Artic World J Pharm Res. 2012. www.wjpr.net
[43] Sharma A, Goyal R, Sharma L. Potential biological efficacy of Pinus plant species against oxidative, inflammatory and microbial disorders. BMC Complement Altern Med. 2016 Jan;16(1):1–8.
[44] Ejiofor EU, Onoja SO, Agwamba EC, Louis H, Onyedikachi UB, Onwuasoanya WE, et al. Computational, chemical profile, in vitro antioxidant, hypoglycaemic, and anti inflammatory activity of hexane extract of some selected dark green vegetables. Proc Indian Natl Sci Acad. 2023;89:386–400. doi: 10.1007/s43538-023-00169-7.
[45] Shraim AM, Ahmed TA, Rahman MM, Hijji YM. Determination of total flavonoid content by aluminum chloride assay: A critical evaluation. LWT. 2021 Oct;150:111932.
[46] Davis AR, Fish WW, Perkins-Veazie P. A rapid spectrophotometric method for analyzing lycopene content in tomato and tomato products. Postharvest Biol Technol. 2003 Jun;28(3):425–30.
[47] Alam MA, Juraimi AS, Rafii MY, Abdul Hamid A, Aslani F, Hasan MM, et al. Evaluation of antioxidant compounds, antioxidant activities, and mineral composition of 13 collected purslane (*Portulaca oleracea* L.) accessions. Biomed Res Int. 2014;2014.
[48] Li L, Long W, Wan X, Ding Q, Zhang F, Wan D. Studies on quantitative determination of total alkaloids and berberine in five origins of crude medicine "Sankezhen." J Chromatogr Sci. 2015 Feb 53(2):307–11. doi: 10.1093/chromsci/bmu060 [cited 2023 Jul 7]
[49] Hussain MB, Ahmad RS, Waheed M, Rehman TU, Majeed M, Khan MU, et al. Extraction and characterization of lycopene from tomato and tomato products. Russ J Agric Socioecon Sci. 2017 Mar;63(3):195–202.
[50] Barchan A, Bakkali M, Arakrak A, Pagán R, Laglaoui A. The effects of solvents polarity on the phenolic contents and antioxidant activity of three Mentha species extracts. Int J Curr Microbiol App Sci. 2014;11:3. http://www.ijcmas.com
[51] Lorence A, Nessler CL. Camptothecin, over four decades of surprising findings. Phytochemistry 2004;65(20):2735–49.
[52] Petros AM, Medek A, Nettesheim DG, Kim DH, Yoon HS, Swift K, et al. Solution structure of the antiapoptotic protein bcl-2. Proc Natl Acad Sci U S A. 2001;98(6):3012–7.
[53] Garner TP, Reyna DE, Priyadarshi A, Chen HC, Li S, Wu Y, et al. An autoinhibited dimeric form of BAX regulates the BAX activation pathway. Mol Cell. 2016 Aug;63(3):485–97.
[54] Tople MS, Patel NB, Patel PP, Purohit AC, Ahmad I, Patel H. An in silico-in vitro antimalarial and antimicrobial investigation of newer 7-chloroquinoline based Schiff-bases. J Mol Struct. 2023 Jan;1271:1271.
[55] Aljuhani A, Ahmed HEA, Ihmaid SK, Omar AM, Althagfan SS, Alahmadi YM, et al. In vitro and computational investigations of novel synthetic carboxamide-linked pyridopyrrolopyrimidines with potent activity as SARS-CoV-2-MPro inhibitors. RSC Adv. 2022;12(41):26895–907.
[56] Radwan HA, Ahmad I, Othman IMM, Gad-Elkareem MAM, Patel H, Aouadi K, et al. Design, synthesis, in vitro anticancer and antimicrobial evaluation, SAR analysis, molecular docking and dynamic simulation of new pyrazoles, triazoles and pyridazines based isoxazole. J Mol Struct. 2022;1264:133312.
[57] Ghosh S, Das S, Ahmad I, Patel H. In silico validation of anti-viral drugs obtained from marine sources as a potential target against SARS-CoV-2 Mpro. J Indian Chem Soc. 2021;98(12):100272.
[58] Minitab Inc. Minitab17. Minitab Inc; 2013. www.mintab.com/assistant. (online)
[59] Ayogu JI, Odoh AS. Prospects and therapeutic applications of cardiac glycosides in cancer remediation. ACS Comb Sci. 2020 Nov;22(11):543–53. doi: 10.1021/acscombsci.0c00082.
[60] Rabi T, Bishayee A. Terpenoids and breast cancer chemoprevention. Breast Cancer Res Treat. 2009;115(2):223–39. doi: 10.1007/s10549-008-0118-y.
[61] Ogundipe A, Adetuyi B, Iheagwam F, Adefoyeke K, Olugbuyiro J, Ogunlana O, et al. In vitro experimental assessment of ethanolic extract of moringa oleifera leaves as an α-amylase and α-lipase inhibitor. Genet Res. 2022;2022:1–8.
[62] Heinrich M, Mah J, Amirkia V. Alkaloids used as medicines: Structural phytochemistry meets biodiversity—An update and forward look. Molecules. 2021;26:1836.

[63] Taiwo EA, Abdulkareem TT, Fajemisin EA. The nutraceutical potential of carrots carotenoids in chronic eyes defects (CEDs): A review; 2021. https://ssrn.com/abstract = 3885012
[64] Mariya A, Hadiza Haruna A, Zakari Babangida A. Phytochemical Analysis of Some Selected Indigenous Fruits Collected from Lokogoma-Abuja, Nigeria. J Dis Medicinal Plants. 2020;6(2):50–5.
[65] Bahanla Oboulbiga E. Assessment of the content of β-carotene, lycopene and total phenolic of 45 varieties of tomatoes (*Solanum lycopersicum* L.). J Food Nutr Sci. 2018;6(3):82.
[66] Przybylska S, Tokarczyk G. Lycopene in the prevention of cardiovascular diseases. Int J Mol Sci. 2022;23(4):1957. https://www.mdpi.com/1422-0067/23/4/1957.
[67] Emmanuel EU, Onagbonfeoana ES, Chinedu NP, Chibuike AO, Edith OC, Chioma I, et al. Ameliorative effect of methanol extract of Telfairia occidentalis Hook. and Amaranthus hybridus Linn. Against cadmium induced oxidative stress in rats. J Appl Pharm Sci. 2017;7(9):109–15.
[68] Pandya D. Standardization of solvent extraction process for lycopene extraction from tomato pomace. J Appl Biotechnol Bioeng. 2017 Jan;2(1):12–6.
[69] Mirahmadi M, Azimi-Hashemi S, Saburi E, Kamali H, Pishbin M, Hadizadeh F. Potential inhibitory effect of lycopene on prostate cancer. Biomed Pharmacother. 2020;129:110459.
[70] Nguyen ML, Schwartz SJ. Lycopene: chemical and biological properties. Food Technol. 1999;53(2):38–45.
[71] Kerna NA. A global health preventive medicine overture: lycopene as an anticancer and carcinopreventive agent in the deterrence of cervical cancer liking lycopene. SM Preventive Med Public Health. 2018;2(2):1–5.
[72] Zhuang E, Uchio E, Lilly M, Zi X, Fruehauf JP. A phase II study of docetaxel plus lycopene in metastatic castrate resistant prostate cancer. Biomed Pharmacother. 2021;143:112226.
[73] Socaci SA, Socaciu C, Mureşan C, Fărcaş A, Tofană M, Vicaş S, et al. Chemometric discrimination of different tomato cultivars based on their volatile fingerprint in relation to lycopene and total phenolics content. Phytochem Anal. 2014;25(2):161–9. https://analyticalsciencejournals.onlinelibrary.wiley.com/doi/abs/10.1002/pca.2483
[74] Paul RK, Ahmad I, Patel H, Kumar V, Raza K. Phytochemicals from Amberboa ramosa as potential DPP-IV inhibitors for the management of Type-II diabetes mellitus: Inferences from in-silico investigations. J Mol Struct. 2023;1271:134045.
[75] Pandey R, Dubey I, Ahmad I, Mahapatra DK, Patel H, Kumar P. In silico study of some dexamethasone analogs and derivatives against SARs-CoV-2 target: A cost-effective alternative to remdesivir for various COVID phases. Curr Chin Sci. 2022;2(4):294–309.
[76] Puri S, Ahmad I, Patel H, Kumar K, Juvale K. Evaluation of oxindole derivatives as a potential anticancer agent against breast carcinoma cells: In vitro, in silico, and molecular docking study. Toxicol Vitro. 2023;86:105517.
[77] Abdelgawad MA, Oh JM, Parambi DGT, Kumar S, Musa A, Ghoneim MM, et al. Development of bromo-and fluoro-based α, β-unsaturated ketones as highly potent MAO-B inhibitors for the treatment of Parkinson's disease. J Mol Struct. 2022;1266:133545.